Repression of Cell Differentiation by a cis-Acting lincRNA in Fission Yeast

Fauquenoy, Sylvain; Migeot, Valerie; Finet, Olivier; Yague-Sanz, Carlo; Khorosjutina, Olga; Ekwall, Karl; Hermand, Damien

Published in:
Current Biology

DOI:
10.1016/j.cub.2017.12.048

Publication date:
2018

Document Version
Publisher's PDF, also known as Version of record

Article

Current Biology

Repression of Cell Differentiation by a *cis*-Acting lincRNA in Fission Yeast

Highlights

- A lincRNA is transcribed divergently to the master regulator of cell differentiation
- The *rse1* lincRNA represses the transcription of the neighboring *ste11*
- *rse1* interacts with and recruits a repressive complex to the promoter of *ste11*

Authors

Sylvain Fauquenoy, Valerie Migeot, Olivier Finet, Carlo Yague-Sanz, Olga Khorosjutina, Karl Ekwall, Damien Hermand

Correspondence

damien.hermand@unamur.be

In Brief

Fauquenoy et al. report the first example of a yeast long intergenic non-coding RNA (lincRNA) that regulates the expression of the neighboring *ste11* gene through scaffolding of a repressive complex. This constitutes an RNA-based mechanism of repression of cell differentiation.

Fauquenoy et al., 2018, Current Biology *28*, 383–391
February 5, 2018
https://doi.org/10.1016/j.cub.2017.12.048

CellPress

Current Biology
Article

Repression of Cell Differentiation by a *cis*-Acting lincRNA in Fission Yeast

Sylvain Fauquenoy,[1] Valerie Migeot,[1] Olivier Finet,[1] Carlo Yague-Sanz,[1] Olga Khorosjutina,[2] Karl Ekwall,[2] and Damien Hermand[1,3,*]
[1]URPHYM-GEMO, The University of Namur, rue de Bruxelles, 61, Namur 5000 Belgium
[2]Karolinska Institut, Alfred Nobels Allee 8, Huddinge 171 77, Sweden
[3]Lead Contact
*Correspondence: damien.hermand@unamur.be
https://doi.org/10.1016/j.cub.2017.12.048

SUMMARY

The cell fate decision leading to gametogenesis requires the convergence of multiple signals on the promoter of a master regulator. In fission yeast, starvation-induced signaling leads to the transcriptional induction of the *ste11* gene, which encodes the central inducer of mating and gametogenesis, known as sporulation. We find that the long intergenic non-coding (linc) RNA *rse1* is transcribed divergently upstream of the *ste11* gene. During vegetative growth, *rse1* directly recruits a Mug187-Lid2-Set1 complex that mediates *cis* repression at the *ste11* promoter through SET3C-dependent histone deacetylation. The absence of *rse1* bypasses the starvation-induced signaling and induces gametogenesis in the presence of nutrients. Our data reveal that the remodeling of chromatin through ncRNA scaffolding of repressive complexes that is observed in higher eukaryotes is a conserved, likely very ancient mechanism for tight control of cell differentiation.

INTRODUCTION

The ability to generate a large range of differentiated cell types imposes a strict regulation of the underlying expression signature to allow diverse and sometimes antagonistic states to coexist. The emergence of chromatin in eukaryotes provides a dynamic and efficient way to control the differentiation programs encoded in the genome. This is exemplified in the fission yeast *Schizosaccharomyces pombe* where developmental genes, which must be silenced during vegetative growth, are often located within heterochromatin islands [1], and their mRNA are targeted for selective degradation [2]. Notably, the formation of heterochromatin at these loci is regulated by environmental cues and developmental signals. Intriguingly, heterochromatin is never detected at the *ste11* locus, which encodes the master regulator of the gametogenesis program [3]. We report here that a chromatin/non-coding RNA-based mechanism is in operation at the *ste11* locus to repress the developmental program.

The past decade has seen the discovery of very large classes of RNAs collectively referred to as long non-coding RNAs (lncRNAs), because they have low or no coding capacity [4–6]. The paradigm that emerged is that lncRNAs are key players in the control of gene expression by coordinating the recruitment of regulatory proteins or localizing them to the target locus [7]. Typically, the mammalian Xist lncRNA scaffolds multiple proteins to enable chromosome-specific transcriptional silencing required for dosage compensation [8]. The flexibility of the lncRNA structure enables the tethering of independent complexes, as shown for the telomerase RNA component TERC that comprises multiple connected domains conferring functional independence [9]. By contrast, it is clear that many lncRNAs are very rapidly degraded by the main 3′ → 5′ RNA degradation machinery [10], the exosome [11], raising the possibility that most are the biologically irrelevant result of transcriptional noise [12].

Genetic dissection, mainly in yeast, has also revealed that the act of transcribing a region of the genome and the associated chromatin modifications and altered dynamics may well be the major regulatory role of the so-called pervasive transcription, excluding a direct role of the produced RNA molecule [13]. Detailed examples of transcriptional interference include the *SRG1* lncRNA, whose transcription into the *SER3* promoter impedes the binding of transcription factor by modulating nucleosome density [14]. The transcription of regulatory regions of the yeast *IME1*, *FLO11*, and *GAL10-GAL1* has similarly been reported to control the induction of these genes, without a decisive role of the lncRNA molecule generated [15–18]. A similar type of mechanism is in operation in fission yeast at the *tgp1* locus that encodes a permease, where lncRNA-mediated transcriptional interference confers drug tolerance [19, 20]. The control of fission yeast cell differentiation by transcriptional interference was also recently documented [21]. By contrast with this list of well-described cases for interference, a single case of an active role of the transcribed lncRNA was reported in the context of fission yeast heterochromatin, where the production of lncRNAs directly recruits a histone deacetylase complex without apparent regulation [22].

Here we report that the repression of the fission yeast differentiation program relies on the negative control of the master regulator Ste11 by the *rse1* lncRNA that functions as a scaffold to recruit a newly identified repressive complex.

RESULTS

The *rse1* lincRNA Represses *ste11* Expression and Gametogenesis

While studying the promoter of *ste11*, we noticed that the expression level was increased when the locus was transferred

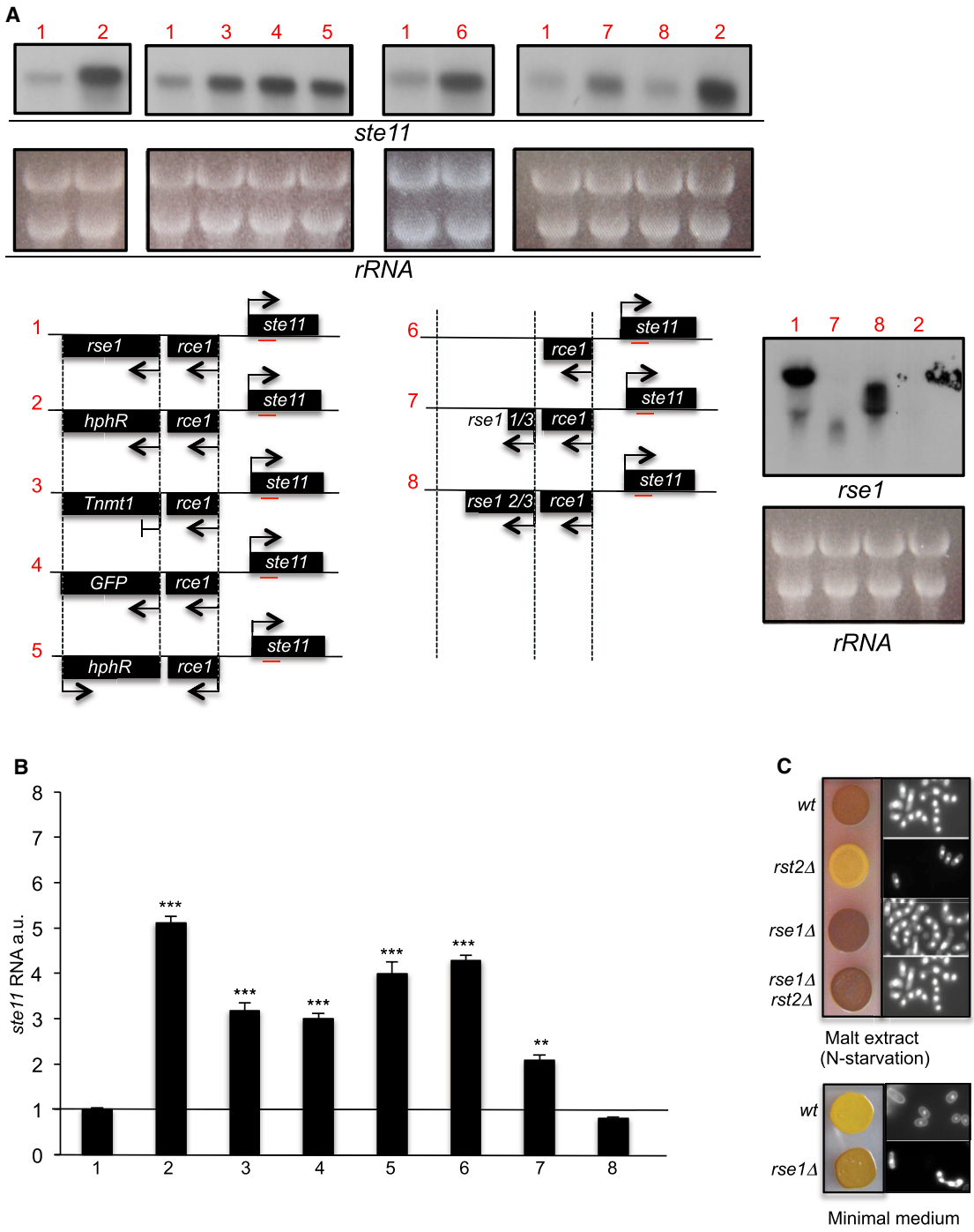

Figure 1. The *rse1* ncRNA Is Required for the Repression of the Neighboring *ste11* Gene

(A) Northern blot analyses of the *ste11* transcript produced in a collection of *rse1* mutants. Ribosomal RNA is shown as a loading control. The probe used is indicated by a red bar in the lower panel that represents the wild-type and altered locus. The right panel shows the northern blot analyses of the *rse1* transcript in the indicated strains, with rRNA shown as a loading control.

(B) qRT-PCR analyses of *ste11* expression in the indicated strains. Each column represents the averaged value ± SEM (n = 3). ***p < 0.001, **p < 0.01, and *p < 0.05, compared with the wild-type homozygous control (Student's t test).

(C) Iodine staining was used to assess the level of gametogenesis in the indicated strains and media. The dark staining results from the presence of gametes. See also Figure S1.

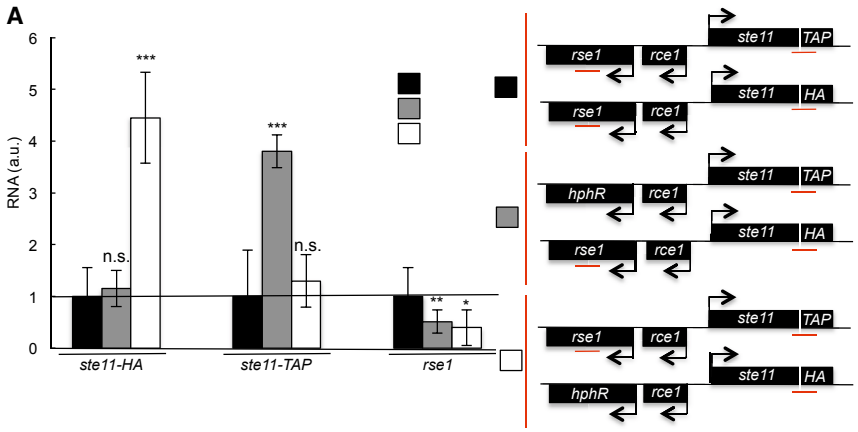

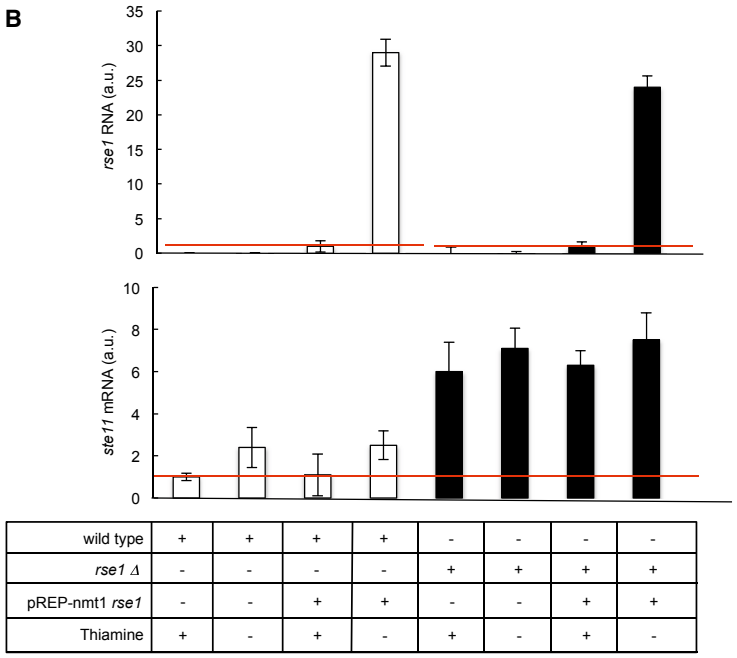

Figure 2. *rse1* Is a *cis*-Acting Non-coding RNA

(A) qRT-PCR analyses of *ste11* and *rse1* expression in strains heterozygous for *rse1* deletion. Both *ste11* alleles are distinguished by the HA and TAP tags and the amplicon is indicated by the red bar. Each column represents the averaged value ± SEM (n = 3). ***p < 0.001, **p < 0.01, and *p < 0.05, compared with the wild-type homozygous control (Student's t test).

(B) *rse1* was expressed from the thiamine-repressed *nmt1* promoter on a pREP plasmid, and the levels of *rse1* and *ste11* were measured by qRT-PCR in a wild-type and an *rse1* deletion strain. Each column represents the averaged value ± SEM (n = 3).

See also Figures S2 and S3.

to a different chromosome (Figure S1A), suggesting that a local repressing mechanism may operate at the endogenous location. Interestingly, a large intergenic non-coding RNA (*SPNCRNA.111*) was annotated upstream of *ste11* on the reverse strand (Figure S1B). Detailed probing of the region by northern blotting revealed that two possibly overlapping RNAs rather than one were expressed from that region (Figure S1C). We named them *rse1* and *rce1* for reasons clarified below. Further analyses indicated that *rse1* is poly-adenylated and 5′/3′ RACE defined it as a 2,336-bp RNA molecule (Figure S2A), which was in agreement with a large-scale analysis of poly-adenylation in fission yeast [23] (Figure S2B). *Sensu stricto*, *rse1* can therefore be defined as a long intergenic non-coding RNA (lincRNA).

We next generated a collection of mutants of this ncRNA, and we analyzed their effect on the neighboring *ste11* gene. The deletion of *rse1* strongly derepressed *ste11*. Although the presence and orientation of the selection marker influenced the level of derepression, the removal of *rse1* in the absence of any molecular scar also increased *ste11* expression (Figures 1A and 1B). The replacement of *rse1* by a transcriptional terminator or by the GFP-coding region similarly led to increased expression of *ste11*. In the latter case, the level of RNA polymerase II (Pol II) present was similar to the wild-type situation (Figure S2C). We concluded that the transcription of the specific piece of DNA corresponding to *rse1*, rather than the act of transcribing the region, was important to maintain basal *ste11* expression. In addition, increasing truncations of *rse1* proportionally affected *ste11*, further supporting that the *rse1* RNA plays an active role in the repression process.

The absence of *rse1* bypassed the requirement of Rst2, a key transcriptional activator of *ste11*, for induction upon starvation, and it led to detectable gametogenesis in rich medium where it is normally repressed (Figure 1C). Microarray analysis of the *rse1* deletion strain confirmed an induction of the gametogenesis program (Data S1; Figure S3A), which was also quantitatively demonstrated (Figure S3B). These evidences led us to name this ncRNA repressor of *ste11* expression (*rse1*).

The *rse1* lincRNA Functions as a *cis*-Acting lincRNA to Repress the Transcription of *ste11*

We next constructed and analyzed a set of heterozygous diploid strains lacking one allele of *rse1*, and we observed that the lincRNA exerts its repressive effect specifically on the neighboring *ste11* allele (Figure 2A), which indicates that it behaves as a *cis*-acting ncRNA. Consistent with a local action of *rse1*, we found that plasmid-borne expression of *rse1*, despite reaching a high level, had no effect on *ste11* expression (Figure 2B).

We investigated the effect of *rse1* deletion on the level of Pol II and the occupancy of histone H3 over the entire locus. Cells lacking *rse1* had an increased Pol II level over the *ste11* transcribed unit and a strongly decreased occupancy of H3 at the *ste11* promoter (Figures 3A and 3B). In addition, H3 present

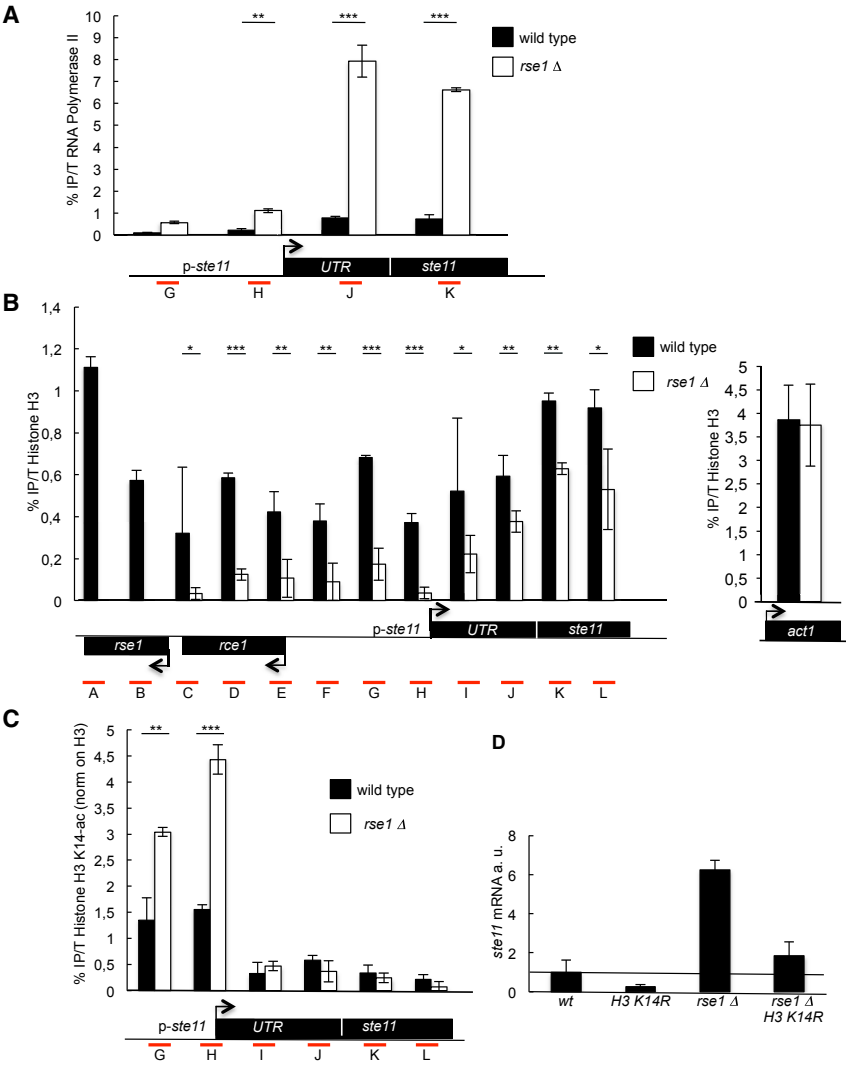

Figure 3. The Absence of *rse1* Results in an Increased Level of Pol II Occupancy and Hyperacetylation at the *ste11* Promoter

(A) ChIP experiment to measure the occupancy of Pol II at the *ste11* locus in the indicated strains using indicated amplicons. Each column represents the averaged value ± SEM (n = 3). ***p < 0.001, **p < 0.01, and *p < 0.05, compared with the wild-type control (Student's t test).

(B) ChIP experiment to measure the occupancy of H3 at the *ste11* and *act1* loci in the indicated strains. Each column represents the averaged value ± SEM (n = 3). ***p < 0.001, **p < 0.01, and *p < 0.05, compared with the wild-type control (Student's t test).

(C) ChIP experiment to measure the occupancy of acetylated K14 H3 normalized on total H3 at the *ste11* locus in the indicated strains. Each column represents the averaged value ± SEM (n = 3). ***p < 0.001, **p < 0.01, and *p < 0.05, compared with the wild-type control (Student's t test).

(D) The level of the *ste11* transcript was determined by qRT-PCR in the indicated strains. Each column represents the averaged value ± SEM (n = 2).

See also Figure S3.

over the *ste11* promoter region, but not the open reading frame (ORF), were highly acetylated (Figure 3C), likely by the SAGA complex [24]. These data support that a transcriptional induction of *ste11* results from the absence of *rse1*. Quantitative analyses of *ste11* mRNA level indicated that the hyperacetylation of H3 was required for derepression, as shown by the fact that an H3K14R mutant, which lacks one major site of acetylation, markedly counteracted the effect of *rse1* deletion (Figure 3D).

The *rse1* lincRNA Directly Binds Mug187 and Is Required to Recruit a Mug187-Lid2-Set1 Complex to the Promoter of *ste11*

We next hypothesized that *rse1* may act in a complex with effector proteins, as observed for an increasing number of lincRNAs in higher eukaryotes [4]. We adapted the chromatin isolation by RNA purification (ChIRP) protocol [25] to yeast to test this possibility (Figure S4). Although a set of hits including RNA-binding proteins was specifically purified with *rse1*, we obtained a low number of peptides, excluding robustly reproducible analyses. Nevertheless, we considered the conserved Mug187 protein as an interesting candidate because its level of expression is regulated by environmental growth conditions [26] and its deletion was reported to result in derepression of *ste11* [27]. We therefore tested a direct interaction between *rse1* and Mug187 using more sensitive methods. We performed an RNA immunoprecipitation (RIP) experiment that showed coprecipitation of Mug187 with *rse1*, but not with the *act1* mRNA or the *snR30* non-coding RNA (Figure 4A). We asked whether Mug187 could directly interact with *rse1* using an *in vitro* pull-down assay, which revealed a direct interaction (Figure 4B). In addition, Mug187 chipped at the *rse1-ste11* locus in a manner dependent on *rse1* (Figure 4C).

We next sought to investigate the mechanistic details of the *rse1*-Mug187 repression of *ste11*, and we performed a two-hybrid screen to identify physical partners of Mug187. The screen repetitively identified the JmjC domain containing protein Lid2 (Figure S5), and the analysis of overlapping interacting fragments delineated a short region of Lid2 corresponding to the second plant homeodomain (PHD) finger as necessary and sufficient for the interaction with Mug187 (Figure S5). Lid2 is an essential H3K4me3 demethylase, homolog of the *Drosophila* Trithorax protein Lid and mammalian transcriptional regulator RBP2. Lid2 interacts with the Set1 H3K4 methyltransferase through its JmjC domain (Figure 4D), and it was shown to be necessary for the recruitment of Set1 to euchromatin [28]. We found that a version of Lid2 that lacks the PHD2 finger required for the interaction with Mug187 is viable and stable (Figure 4E), which allowed us to specifically dissect the role of the Lid2-Mug187 interaction. Lid2 robustly chipped at the *ste11* promoter

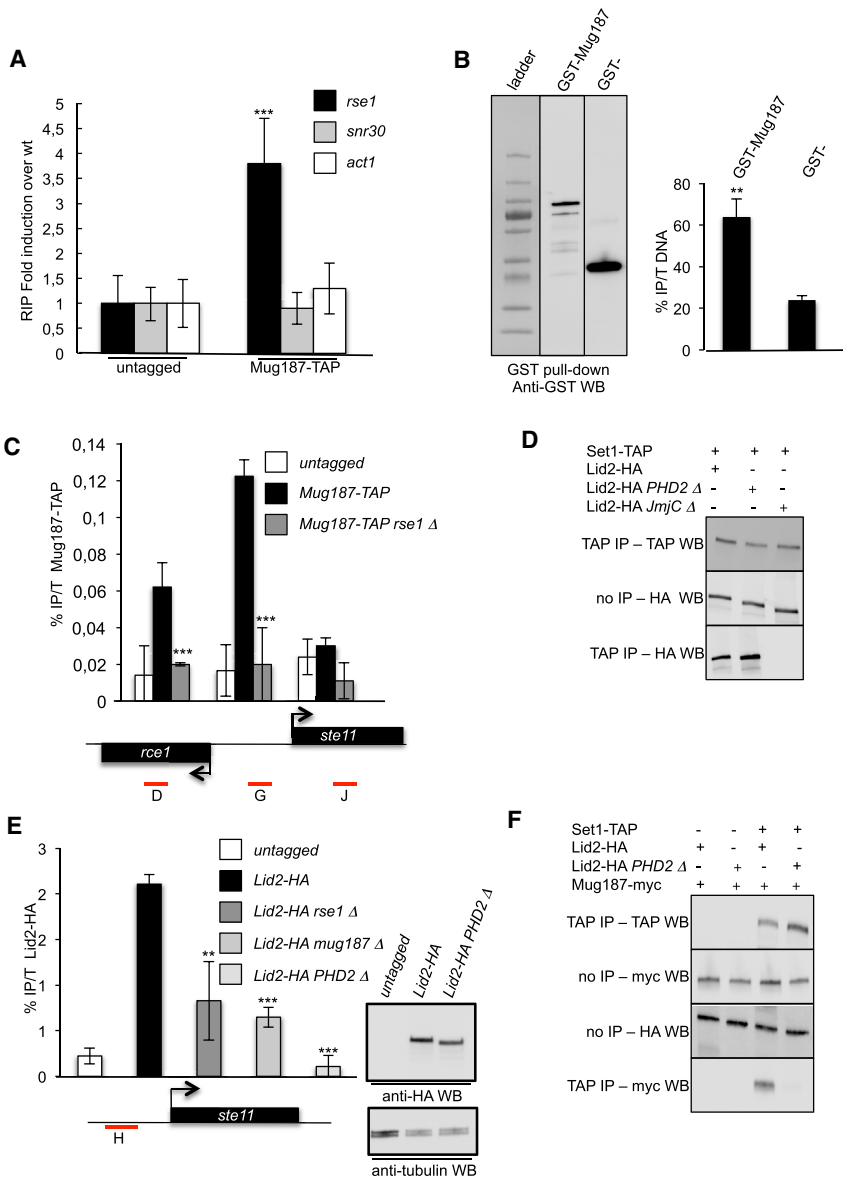

Figure 4. Mug187 Associates with *rse1* and Forms a Complex with Lid2 and Set1

(A) RIP experiments measuring the enrichment of Mug187-TAP at *rse1*, *snR30* (small nucleolar RNA [snoRNA]), and *act1* (mRNA) transcripts. Each column represents the averaged value ± SEM (n = 3). ***p < 0.001, **p < 0.01, and *p < 0.05, compared with the untagged strain (Student's t test).

(B) GST-Mug187 or GST pull-down of *in vitro*-transcribed *rse1* to detect a direct interaction The percentage of precipitated versus total *rse1* is presented. Each column represents the averaged value ± SEM (n = 3). ***p < 0.001, **p < 0.01, and *p < 0.05, compared with the GST control (Student's t test).

(C) ChIP experiment to measure the occupancy of Mug187-TAP at the *ste11* promoter in the indicated strains. Each column represents the averaged value ± SEM (n = 3). ***p < 0.001, **p < 0.01, and *p < 0.05, compared with the Mug187-TAP strain (Student's t test).

(D) Co-immunoprecipitation of Set1 with mutants of Lid2 shows that the JmjC domain is required for the interaction while the PHD2 domain is not. Co-immunoprecipitations and western blots were performed as indicated.

(E) ChIP experiment to measure the occupancy of Lid2-HA at the *ste11* promoter in the indicated strains. Each column represents the averaged value ± SEM (n = 3). ***p < 0.001, **p < 0.01, and *p < 0.05, compared with the Lid2-HA strain (Student's t test). Right panel: western blot analysis of the level and size of Lid2-HA (wild-type [WT] and *PHD2 Δ*) is shown. The level of tubulin is shown as a loading control.

(F) Co-immunoprecipitation of Set1 and Mug187 requires the PHD2 domain of Lid2. Co-immunoprecipitations and western blots were performed as indicated.

See also Figure S4.

in a manner dependent on the presence of *rse1*, Mug187, and the PHD2 finger. Indeed, the removal of the PHD2 finger that mediates the interaction with Mug187 was sufficient to completely abolish the Lid2 chromatin immunoprecipitation (ChIP) signal (Figure 4E) while maintaining the interaction with Set1 (Figure 4D). Moreover, the ability of Set1 to co-immunoprecipitate Mug187 was dependent on the PHD2 of Lid2 (Figure 4F). Importantly, the occupancy of Set1 at the *ste11* promoter, which we have recently shown to play a critical role in the repression of *ste11* expression [29, 30], was also decreased in the absence of *rse1*, Mug187 (Figure 5A), or the PHD2 of Lid2 (Figure 5B). These data are consistent with a model where the *rse1*-Mug187 complex is required to recruit the Lid2-Set1 complex at the *ste11* promoter.

We next investigated how the various players identified above affected the level of expression of *ste11* before and after a developmental signal (nutritional starvation). The absence of *rse1*, Mug187, and Set1 led to *ste11* derepression (Figure 5C). We also confirmed that the deletion of the Hos2 histone deacetylase (HDAC), which is acting downstream of Set1, behaved similarly as we previously reported [29]. Interestingly, the effect of Mug187 was less prominent, which may relate to the fact that the deletion of *mug187* did not completely abolish the recruitment of Lid2 while the removal of the PHD2 finger did (Figure 4E). Consistent with this, the removal of the PHD2 finger also strongly derepressed *ste11* expression (Figure 5C). It is, therefore, possible that additional regulators participate in the repression process.

The Lid2 protein was previously shown to bind Set1 and to display H3K4me3 demethylase activity [28]. We measured the level of H3K4me3 and H3K4me2 at the promoter of *ste11* in various strains. In the absence of *rse1*, *mug187*, or the PHD2 of Lid2, the level of H3K4me3 was reduced (Figure S6A), consistent with the decrease of Set1 observed in the same strains (Figures 5A and 5B).

Compared to H3K4me3, the occupancy of H3K4me2 was low at the promoter of *ste11*, and it may have been slightly increased

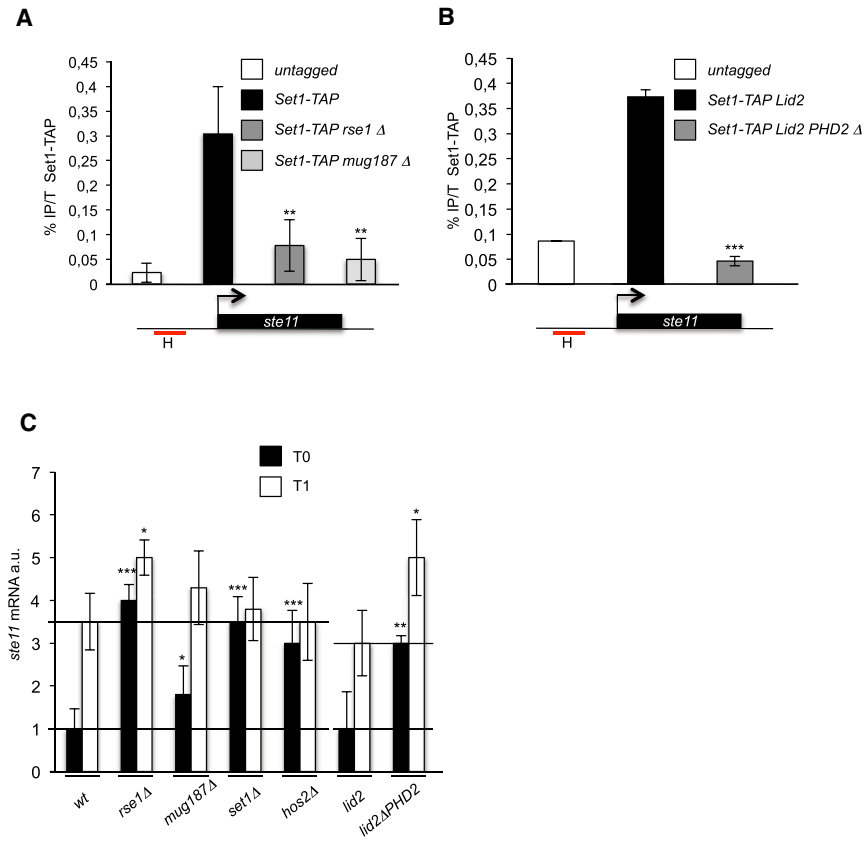

Figure 5. The Recruitment of Set1 and Mug187 at the *ste11* Locus Requires *rse1*

(A) ChIP experiment to measure the occupancy of Set1-TAP at the *ste11* promoter in the indicated strains. Each column represents the averaged value ± SEM (n = 3). ***p < 0.001, **p < 0.01, and *p < 0.05, compared with the Set1-TAP strain (Student's t test).

(B) ChIP experiment to measure the occupancy of Set1-TAP at the *ste11* promoter in the indicated strains. Each column represents the averaged value ± SEM (n = 3). ***p < 0.001, **p < 0.01, and *p < 0.05, compared with the Set1-TAP strain (Student's t test).

(C) The level of the *ste11* transcript was determined by qRT-PCR in the indicated strains before (T0) or after 1 hr of starvation (T1). Each column represents the averaged value ± SEM (n = 3). ***p < 0.001, **p < 0.01, and *p < 0.05, compared with the wild-type control at the same time point (Student's t test). Note that a different control strain is used for testing the *lid2 PHD2 Δ*, as the mutant is expressed from a plasmid in a *lid2* deletion background.

See also Figure S5.

in the absence of *rse1*, *mug187*, or the PHD2 of Lid2 (Figure S6B).

We next used CRISPR interference [31, 32] using a catalytically inactive Cas9 enzyme to suppress the strand-specific transcription of either *rse1* without affecting the underlying DNA sequence. Targeting *rse1* resulted in its downregulation while the expression of *ste11* was increased, which was reminiscent of the deletion of *rse1*. These data indicate that the underlying DNA sequence of *rse1* is not sufficient to repress *ste11* (Figures 6A and 6B). Interestingly, this experiment also revealed that the induction of *ste11* upon starvation is correlated with a decrease in the level of *rse1*, suggesting an active regulation (see the Discussion).

Taken together, these data support a model where the *rse1* lincRNA actively represses the expression of *ste11* during vegetative growth by promoting the deacetylation of the *ste11* promoter (Figure 6C).

DISCUSSION

In fission yeast, the decision to switch from vegetative growth to gametogenesis induced by poor growth conditions must be taken during the very short (about 10 min) G1 phase of the cell cycle. It relies on the integration of key signaling pathways in the eukaryotic cell, including TOR, PkA, and MAPK at the level of the *ste11* promoter. How this integration occurs at the molecular level is unknown, but it must allow an irreversible switch that occurs only when a threshold is passed, beyond low-level fluctuations of the signaling cascades. We propose that an RNA-dependent, chromatin-based mechanism participates in the maintenance of this threshold by promoting the deacetylation of the promoter of *ste11* when vegetative growth occurs.

In contrast to previous examples of the implication of lncRNAs in the control of protein-coding gene expression in budding yeast [15–18] or fission yeast [19, 20, 33], the specificity of the regulation by *rse1* is that the non-coding RNA is transcribed divergently from its target and directly recruits a repressive complex. We have identified 68 lincRNA/mRNA divergent pairs (Data S2) within the fission yeast genome, and further work may, therefore, reveal a more general occurrence of scaffolding lincRNAs in controlling neighboring genes in fission yeast and higher eukaryotes.

The following data support a direct role of *rse1* in the recruitment of the repressive Mug187-Lid2-Set1 complex at the *ste11* promoter. The deletion of *rse1*, its replacement by the GFP-coding region or a transcriptional terminator, and the strand-specific suppression of its transcription by CRISPRi without modifying the DNA sequence all result in the derepression of *ste11*. Moreover, *rse1* interacts directly with the Mug187 protein both *in vivo* and *in vitro*, and it is required for the efficient recruitment of Set1 and Lid2.

Set1 and Lid2 were previously shown to interact [28, 34], and our data confirm that the interaction is mediated through the JmJC domain. Lid2 was proposed to recruit Set1 independently of its catalytic activity and found to associate with euchromatic regions, suggesting that it may have a role beyond the *ste11* locus. We propose that Mug187 is linking the Lid2-Set1 complex to *rse1* by interacting directly with both. The recruitment of Lid2 and Set1 at the *ste11* locus requires Mug187. However, we notice that the effect of deleting *mug187* on *ste11* expression is weaker than the deletion of its partners, suggesting that another yet unknown RNA-binding protein may participate in the recruitment of the Set1-Lid2 complex at the *ste11* locus.

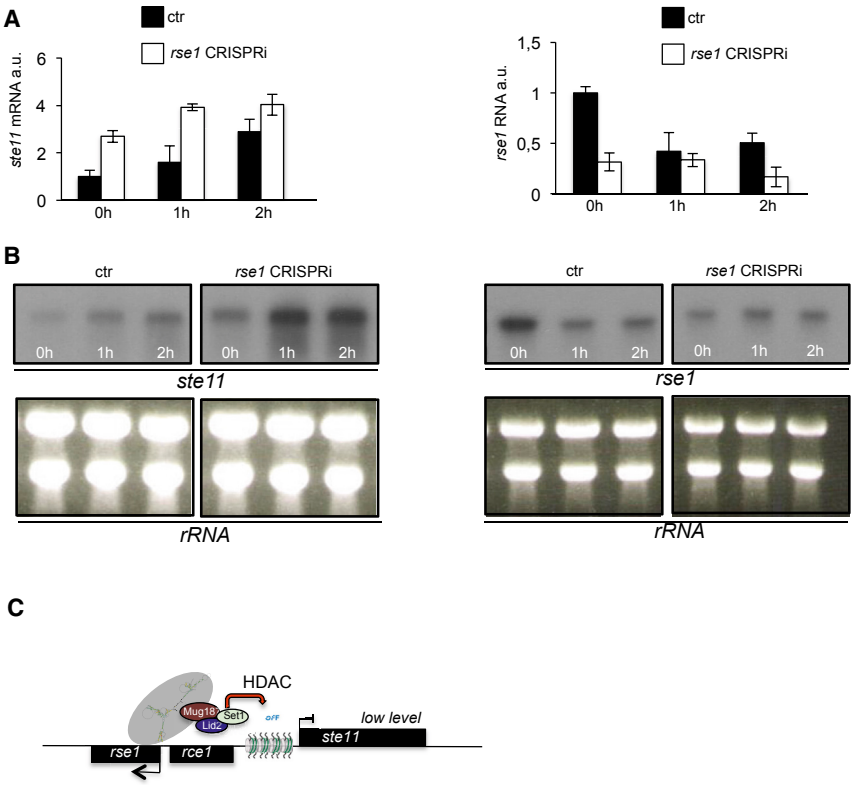

Figure 6. The Underlying DNA Sequence of the *rse1* Locus Is Not Sufficient for Repression of *ste11*

(A) The level of expression of the *ste11* and *rse1* transcripts was determined at the indicated times during the induction of gametogenesis by qRT-PCR. Each column represents the averaged value ± SEM (n = 3). The black square (ctr) indicates that no guide RNA was expressed in the experiment. The empty square (*rse1* CRISPRi) indicates that a guide RNA targeting the non-template strand of the *rse1* transcription unit was expressed (see the STAR Methods for details).

(B) The level of expression of the *ste11* and *rse1* transcripts was determined at the indicated times during the induction of gametogenesis by northern blot analyses. The rRNA is shown as a loading control.

(C) A model of the repression of *ste11* expression by the *rse1* lincRNA. In nutrient-rich conditions, *rse1* expression is high and recruits the Mug187-Lid2-Set1 complex that leads to chromatin deacetylation (by the Hos2 HDAC, not shown) and a high level of H3 at the promoter of *ste11*, resulting in a low level of transcription of *ste11*.

See also Figure S6.

This RNA-binding protein could be Set1 itself, as the protein possesses an RNA recognition motif (RRM) [27].

Our previous work revealed that Set1 is also recruited at the *ste11* promoter through the S5-phosphorylated C-terminal domain (CTD) of Pol II [29, 30, 35], which raised the question of the specificity of the repressive effect of Set1 on only a subset of genes while Set1 and its H3K4 methylation signature constitutes a universal feature of Pol II transcription. We propose that, while the phosphorylated CTD is required for the recruitment of Set1, its maintenance and repressive effect at specific loci, including *ste11*, require additional layers of regulation, including the scaffolding role of *rse1*. A detailed analysis of the genome-wide occupancy of Lid2 and its PHD2-truncated version, together with their effect on Set1, will help to clarify this issue in the future. Interestingly, a repressive role of the Lid2 homolog Rbp2 in the control of cell differentiation was previously reported [36], and it was hypothesized that Rbp2 inhibits differentiation by repressing transcription and participating in a differentiation checkpoint [37], a concept compatible with the model we propose here.

An interesting possibility supported by our previous and current works is that, upon nutritional starvation, the rise of CTD S2P displaces Set1, which would activate the catalytic activity of Lid2 (as Set1 binds the JmjC domain of Lid2), and therefore further decreases the level of H3K4 trimethylation to favor *ste11* induction. Additional work is required in order to test this possibility.

The presence of a second non-coding RNA (tentatively named *rce1* for *rse1* control element) transcribed within the promoter of *rse1* is intriguing, and we are currently investigating if its transcription may participate in the downregulation of *rse1* we observed during starvation (Figures 6A and 6B), maybe through a mechanism of transcriptional interference.

A fundamental aspect of cell differentiation is the conversion of temporary changes in the environmental cues into the expression of a specific genetic program leading to a stable phenotype. Gametogenesis represents a highly coordinated example of differentiation that ensures the shuffling of genetic material, which is expected to participate in cell adaptation and evolution. The existence of highly dynamic RNA-based chromatin mechanisms may have been critical to allow simple eukaryotic organisms to evolve gametogenesis programs. Notably, it was recently reported that some of them closely related to fission yeast, in terms of genome size and complexity, can form complex multicellularity comprising tissue organization and predetermined developmental programs reminiscent of higher eukaryotes [38].

STAR★METHODS

Detailed methods are provided in the online version of this paper and include the following:

- KEY RESOURCES TABLE
- CONTACT FOR REAGENT AND RESOURCE SHARING
- EXPERIMENTAL MODEL AND SUBJECT DETAILS
  - Fission yeast methods
- METHODS DETAILS
  - Northern blot and Q-RT PCR
  - ChIP, RIP and quantitative RT-PCR
  - Microarray experiments
  - Co-IP and *in vitro* GST pull-down assay of RNA

- RACE and poly-A RNA purification
- Chromatin Isolation by RNA precipitation
- Strand-specific CRISPR interference

- QUANTIFICATION AND STATISTICAL ANALYSIS
- DATA AVAILABILITY

SUPPLEMENTAL INFORMATION

Supplemental Information includes six figures and four data files and can be found with this article online at https://doi.org/10.1016/j.cub.2017.12.048.

ACKNOWLEDGMENTS

S.F. was supported by a Marie Curie action of the European Commission. K.E. was supported by grants from The Swedish Cancer Society, The Stockholm County Council, and The Swedish Research Council. D.H. was supported by grants FRFC 2.4510.10, Credit aux chercheurs 1.5.013.09, MIS F.4523.11, and Ceruna and Marie Curie Action. D.H. is a senior FNRS Research Associate.

AUTHOR CONTRIBUTIONS

S.F., V.M., and O.F. performed the experiments. K.E. and O.K. designed and performed the microarray experiments. C.Y.-S. analyzed large datasets. D.H. supervised the work and wrote the manuscript.

DECLARATION OF INTERESTS

The authors declare no competing interests.

Received: September 15, 2017
Revised: October 19, 2017
Accepted: December 20, 2017
Published: January 25, 2018

REFERENCES

1. Zofall, M., Yamanaka, S., Reyes-Turcu, F.E., Zhang, K., Rubin, C., and Grewal, S.I. (2012). RNA elimination machinery targeting meiotic mRNAs promotes facultative heterochromatin formation. Science *335*, 96–100.
2. Hiriart, E., Vavasseur, A., Touat-Todeschini, L., Yamashita, A., Gilquin, B., Lambert, E., Perot, J., Shichino, Y., Nazaret, N., Boyault, C., et al. (2012). Mmi1 RNA surveillance machinery directs RNAi complex RITS to specific meiotic genes in fission yeast. EMBO J. *31*, 2296–2308.
3. Anandhakumar, J., Fauquenoy, S., Materne, P., Migeot, V., and Hermand, D. (2013). Regulation of entry into gametogenesis by Ste11: the endless game. Biochem. Soc. Trans. *41*, 1673–1678.
4. Guil, S., and Esteller, M. (2012). Cis-acting noncoding RNAs: friends and foes. Nat. Struct. Mol. Biol. *19*, 1068–1075.
5. Kung, J.T., Colognori, D., and Lee, J.T. (2013). Long noncoding RNAs: past, present, and future. Genetics *193*, 651–669.
6. Mercer, T.R., and Mattick, J.S. (2013). Structure and function of long noncoding RNAs in epigenetic regulation. Nat. Struct. Mol. Biol. *20*, 300–307.
7. Engreitz, J.M., Ollikainen, N., and Guttman, M. (2016). Long non-coding RNAs: spatial amplifiers that control nuclear structure and gene expression. Nat. Rev. Mol. Cell Biol. *17*, 756–770.
8. Chow, J., and Heard, E. (2009). X inactivation and the complexities of silencing a sex chromosome. Curr. Opin. Cell Biol. *21*, 359–366.
9. Zappulla, D.C., and Cech, T.R. (2004). Yeast telomerase RNA: a flexible scaffold for protein subunits. Proc. Natl. Acad. Sci. USA *101*, 10024–10029.
10. Wyers, F., Rougemaille, M., Badis, G., Rousselle, J.C., Dufour, M.E., Boulay, J., Régnault, B., Devaux, F., Namane, A., Séraphin, B., et al. (2005). Cryptic pol II transcripts are degraded by a nuclear quality control pathway involving a new poly(A) polymerase. Cell *121*, 725–737.
11. Houseley, J., LaCava, J., and Tollervey, D. (2006). RNA-quality control by the exosome. Nat. Rev. Mol. Cell Biol. *7*, 529–539.
12. Struhl, K. (2007). Transcriptional noise and the fidelity of initiation by RNA polymerase II. Nat. Struct. Mol. Biol. *14*, 103–105.
13. Li, B., Carey, M., and Workman, J.L. (2007). The role of chromatin during transcription. Cell *128*, 707–719.
14. Martens, J.A., Laprade, L., and Winston, F. (2004). Intergenic transcription is required to repress the Saccharomyces cerevisiae SER3 gene. Nature *429*, 571–574.
15. Bumgarner, S.L., Dowell, R.D., Grisafi, P., Gifford, D.K., and Fink, G.R. (2009). Toggle involving cis-interfering noncoding RNAs controls variegated gene expression in yeast. Proc. Natl. Acad. Sci. USA *106*, 18321–18326.
16. Bumgarner, S.L., Neuert, G., Voight, B.F., Symbor-Nagrabska, A., Grisafi, P., van Oudenaarden, A., and Fink, G.R. (2012). Single-cell analysis reveals that noncoding RNAs contribute to clonal heterogeneity by modulating transcription factor recruitment. Mol. Cell *45*, 470–482.
17. Houseley, J., Rubbi, L., Grunstein, M., Tollervey, D., and Vogelauer, M. (2008). A ncRNA modulates histone modification and mRNA induction in the yeast GAL gene cluster. Mol. Cell *32*, 685–695.
18. van Werven, F.J., Neuert, G., Hendrick, N., Lardenois, A., Buratowski, S., van Oudenaarden, A., Primig, M., and Amon, A. (2012). Transcription of two long noncoding RNAs mediates mating-type control of gametogenesis in budding yeast. Cell *150*, 1170–1181.
19. Ard, R., and Allshire, R.C. (2016). Transcription-coupled changes to chromatin underpin gene silencing by transcriptional interference. Nucleic Acids Res. *44*, 10619–10630.
20. Ard, R., Tong, P., and Allshire, R.C. (2014). Long non-coding RNA-mediated transcriptional interference of a permease gene confers drug tolerance in fission yeast. Nat. Commun. *5*, 5576.
21. Touat-Todeschini, L., Shichino, Y., Dangin, M., Thierry-Mieg, N., Gilquin, B., Hiriart, E., Sachidanandam, R., Lambert, E., Brettschneider, J., Reuter, M., et al. (2017). Selective termination of lncRNA transcription promotes heterochromatin silencing and cell differentiation. EMBO J. *36*, 2626–2641.
22. Marina, D.B., Shankar, S., Natarajan, P., Finn, K.J., and Madhani, H.D. (2013). A conserved ncRNA-binding protein recruits silencing factors to heterochromatin through an RNAi-independent mechanism. Genes Dev. *27*, 1851–1856.
23. Mata, J. (2013). Genome-wide mapping of polyadenylation sites in fission yeast reveals widespread alternative polyadenylation. RNA Biol. *10*, 1407–1414.
24. Helmlinger, D., Marguerat, S., Villén, J., Gygi, S.P., Bähler, J., and Winston, F. (2008). The S. pombe SAGA complex controls the switch from proliferation to sexual differentiation through the opposing roles of its subunits Gcn5 and Spt8. Genes Dev. *22*, 3184–3195.
25. Chu, C., Qu, K., Zhong, F.L., Artandi, S.E., and Chang, H.Y. (2011). Genomic maps of long noncoding RNA occupancy reveal principles of RNA-chromatin interactions. Mol. Cell *44*, 667–678.
26. Wilhelm, B.T., Marguerat, S., Watt, S., Schubert, F., Wood, V., Goodhead, I., Penkett, C.J., Rogers, J., and Bähler, J. (2008). Dynamic repertoire of a eukaryotic transcriptome surveyed at single-nucleotide resolution. Nature *453*, 1239–1243.
27. Hasan, A., Cotobal, C., Duncan, C.D., and Mata, J. (2014). Systematic analysis of the role of RNA-binding proteins in the regulation of RNA stability. PLoS Genet. *10*, e1004684.
28. Li, F., Huarte, M., Zaratiegui, M., Vaughn, M.W., Shi, Y., Martienssen, R., and Cande, W.Z. (2008). Lid2 is required for coordinating H3K4 and H3K9 methylation of heterochromatin and euchromatin. Cell *135*, 272–283.
29. Materne, P., Anandhakumar, J., Migeot, V., Soriano, I., Yague-Sanz, C., Hidalgo, E., Mignion, C., Quintales, L., Antequera, F., and Hermand, D. (2015). Promoter nucleosome dynamics regulated by signalling through the CTD code. eLife *4*, e09008.

30. Materne, P., Vázquez, E., Sánchez, M., Yague-Sanz, C., Anandhakumar, J., Migeot, V., Antequera, F., and Hermand, D. (2016). Histone H2B ubiquitylation represses gametogenesis by opposing RSC-dependent chromatin remodeling at the ste11 master regulator locus. eLife *5*, e13500.

31. Lenstra, T.L., Coulon, A., Chow, C.C., and Larson, D.R. (2015). Single-Molecule Imaging Reveals a Switch between Spurious and Functional ncRNA Transcription. Mol. Cell *60*, 597–610.

32. Larson, M.H., Gilbert, L.A., Wang, X., Lim, W.A., Weissman, J.S., and Qi, L.S. (2013). CRISPR interference (CRISPRi) for sequence-specific control of gene expression. Nat. Protoc. *8*, 2180–2196.

33. Shah, S., Wittmann, S., Kilchert, C., and Vasiljeva, L. (2014). lncRNA recruits RNAi and the exosome to dynamically regulate pho1 expression in response to phosphate levels in fission yeast. Genes Dev. *28*, 231–244.

34. Roguev, A., Schaft, D., Shevchenko, A., Aasland, R., Shevchenko, A., and Stewart, A.F. (2003). High conservation of the Set1/Rad6 axis of histone 3 lysine 4 methylation in budding and fission yeasts. J. Biol. Chem. *278*, 8487–8493.

35. Coudreuse, D., van Bakel, H., Dewez, M., Soutourina, J., Parnell, T., Vandenhaute, J., Cairns, B., Werner, M., and Hermand, D. (2010). A gene-specific requirement of RNA polymerase II CTD phosphorylation for sexual differentiation in S. pombe. Curr. Biol. *20*, 1053–1064.

36. van Oevelen, C., Wang, J., Asp, P., Yan, Q., Kaelin, W.G., Jr., Kluger, Y., and Dynlacht, B.D. (2008). A role for mammalian Sin3 in permanent gene silencing. Mol. Cell *32*, 359–370.

37. Benevolenskaya, E.V., Murray, H.L., Branton, P., Young, R.A., and Kaelin, W.G., Jr. (2005). Binding of pRB to the PHD protein RBP2 promotes cellular differentiation. Mol. Cell *18*, 623–635.

38. Nagy, L.G. (2017). Evolution: Complex Multicellular Life with 5,500 Genes. Curr. Biol. *27*, R609–R612.

39. Bamps, S., Westerling, T., Pihlak, A., Tafforeau, L., Vandenhaute, J., Mäkelä, T.P., and Hermand, D. (2004). Mcs2 and a novel CAK subunit Pmh1 associate with Skp1 in fission yeast. Biochem. Biophys. Res. Commun. *325*, 1424–1432.

40. Devos, M., Mommaerts, E., Migeot, V., van Bakel, H., and Hermand, D. (2015). Fission yeast Cdk7 controls gene expression through both its CAK and C-terminal domain kinase activities. Mol. Cell. Biol. *35*, 1480–1490.

41. Fersht, N., Hermand, D., Hayles, J., and Nurse, P. (2007). Cdc18/CDC6 activates the Rad3-dependent checkpoint in the fission yeast. Nucleic Acids Res. *35*, 5323–5337.

42. Bauer, F., and Hermand, D. (2012). A coordinated codon-dependent regulation of translation by Elongator. Cell Cycle *11*, 4524–4529.

43. Guiguen, A., Soutourina, J., Dewez, M., Tafforeau, L., Dieu, M., Raes, M., Vandenhaute, J., Werner, M., and Hermand, D. (2007). Recruitment of P-TEFb (Cdk9-Pch1) to chromatin by the cap-methyl transferase Pcm1 in fission yeast. EMBO J. *26*, 1552–1559.

44. Lenglez, S., Hermand, D., and Decottignies, A. (2010). Genome-wide mapping of nuclear mitochondrial DNA sequences links DNA replication origins to chromosomal double-strand break formation in Schizosaccharomyces pombe. Genome Res. *20*, 1250–1261.

45. Rougemaille, M., Braun, S., Coyle, S., Dumesic, P.A., Garcia, J.F., Isaac, R.S., Libri, D., Narlikar, G.J., and Madhani, H.D. (2012). Ers1 links HP1 to RNAi. Proc. Natl. Acad. Sci. USA *109*, 11258–11263.

46. Hermand, D., Pihlak, A., Westerling, T., Damagnez, V., Vandenhaute, J., Cottarel, G., and Mäkelä, T.P. (1998). Fission yeast Csk1 is a CAK-activating kinase (CAKAK). EMBO J. *17*, 7230–7238.

47. Tafforeau, L., Le Blastier, S., Bamps, S., Dewez, M., Vandenhaute, J., and Hermand, D. (2006). Repression of ergosterol level during oxidative stress by fission yeast F-box protein Pof14 independently of SCF. EMBO J. *25*, 4547–4556.

48. Yamaji, Y., Kobayashi, T., Hamada, K., Sakurai, K., Yoshii, A., Suzuki, M., Namba, S., and Hibi, T. (2006). In vivo interaction between Tobacco mosaic virus RNA-dependent RNA polymerase and host translation elongation factor 1A. Virology *347*, 100–108.

49. Chu, C., Zhang, Q.C., da Rocha, S.T., Flynn, R.A., Bharadwaj, M., Calabrese, J.M., Magnuson, T., Heard, E., and Chang, H.Y. (2015). Systematic discovery of Xist RNA binding proteins. Cell *161*, 404–416.

50. Jacobs, J.Z., Ciccaglione, K.M., Tournier, V., and Zaratiegui, M. (2014). Implementation of the CRISPR-Cas9 system in fission yeast. Nat. Commun. *5*, 5344.

51. Howe, F.S., Russell, A., Lamstaes, A.R., El-Sagheer, A., Nair, A., Brown, T., and Mellor, J. (2017). CRISPRi is not strand-specific at all loci and redefines the transcriptional landscape. eLife *6*, e29878.

STAR★METHODS

KEY RESOURCES TABLE

REAGENT or RESOURCE	SOURCE	IDENTIFIER
Antibodies		
anti-HA	Sigma	H6908
PAP	Sigma	P1291
Ant-GST	Sigma	T5168
Anti-PolII	Covance	MMS-126R
Anti-H3	Abcam	1791
Anti-H3 K14-ac	Millipore	07-353
Anti-H3K4me3	Millipore	07-473
Anti-H3K4me2	Millipore	07-030
Critical Commercial Assays		
Q5 mutagenesis kit	New Englands Biolabs	E0554
RNeasy	QIAGEN	74104
RNA-to-cDNA	Thermo	4387406
M-MLV RT	Invitrogen	28025013
Dynabeads	Thermo	11041
GST purification kit	Thermo	25239
Ribomax T7 *in vitro* transcription kit	Promega	P1300
SMARTer RACE	Clonetech	634858
MyOne streptavine beads	Thermo	65601
Deposited Data		
Microarray data	GEO	GSE89825
Experimental Models: Organisms/Strains		
Fission yeast strains	N/A	See Data S4
Oligonucleotides		
Oligonucleotides	IDT	See Data S3
Software and Algorithms		
GraphPad Prism	N/A	https://www.graphpad.com/scientific-software/prism/
PodBat	N/A	https://omictools.com/podbat-tool
ApE	N/A	http://biologylabs.utah.edu/jorgensen/wayned/ape/

CONTACT FOR REAGENT AND RESOURCE SHARING

Further information and requests for resources and reagents should be directed to and will be fulfilled by the Lead Contact, Damien Hermand (Damien.Hermand@unamur.be).

EXPERIMENTAL MODEL AND SUBJECT DETAILS

Fission yeast methods

Wild-type and mutant strains listed in Data S4 were grown at 32°C in rich YES medium or minimal EMM medium as indicated. For starvation, cells were shifted by filtration from EMM to EMM lacking nitrogen or from YES (2% glucose) to YES (0.1% glucose) as indicated. Fission yeast growth, gene targeting, including locus-specific integration, and mating were performed using classical methods [39–41]. Western blot were performed with anti-HA (Sigma #H6908), PAP (Sigma #P1291) and anti-GST (Sigma #T5168) antibodies. Iodine staining was performed by exposing 48 hours crosses to Iodine [42]. Mutagenesis of *lid2* were performed using the Q5 mutagenesis kit of New England Biolabs. The Two-hybrid screen was performed by Hybrigenics following their protocol (https://www.hybrigenics-services.com/contents/our-services/discover/ultimate-y2h-2).

Except stated otherwise, the strain indicated as *rse1Δ* is strain #993. All *rse1* mutants were generated using the 5-FOA counter-selection method following the replacement of *rse1* by *ura4*. Consequently, the *hphR* marker, the GFP coding region and the *nmt1* terminator precisely replace *rse1*. The strains maintaining 1/3 and 2/3 of *rse1* were constructed similarly. Strain #7 in Figure 1A retains the first 985 bp of *rse1* and strain #8 retains the first 1697 bp of *rse1* whose full length reaches 2336 bp.

METHODS DETAILS

Northern blot and Q-RT PCR

Total RNA was prepared by phenol extraction [43] and purified on QIAGEN RNeasy. Total RNA (15 to 30 μg) was separated on gel and transferred on nitrocellulose. Hybridization of a multiprimed labeled probe covering indicated positions was performed overnight at 42°C. Q-RT-PCR was performed using the ABI high capacity RNA-to-cDNA following the instructions of the manufacturer. The untreated sample was used as a reference and the *act1* mRNA was used for normalization. In all Q-RT-PCR experiments, each column represents the averaged value ± SEM. The number of biological replicates is indicated in the legend (n). Statistical significance was assessed using Student's t test, which tested the hypothesis that the mean fold-enrichment was greater than 1 (***$p < 0.001$; ** $p < 0.01$; *$p < 0.05$).

ChIP, RIP and quantitative RT-PCR

Chromatin Immunoprecipitations were performed using a Bioruptor (Diagenode) and Dynabeads (Invitrogen) [44]. Precipitated DNA was purified on QIAGEN. Quantitative RT-PCR was performed using the ABI high capacity RNA-to-cDNA. The untreated sample / untagged strain was used as a reference and the *act1* mRNA was used for normalization. Antibodies used in ChIP were anti-Pol II (Covance #MMS-126R), anti-H3 (Abcam #1791), anti-H3 K14-ac (Millipore #07-353), anti-HA (Sigma #H6908), anti H3K4me3 (Millipore 07-473), anti-H3K4me2 (Millipore 07-030) and PAP (Sigma #P1291). For all ChIP experiments, each column represents the mean percentage immunoprecipitation value ± SEM. The number of biological replicates is indicated in the legend (n). Statistical significance was assessed using Student's t test, which tested the hypothesis that the mean fold-enrichment was greater than 1 (***$p < 0.001$; ** $p < 0.01$; *$p < 0.05$).

RNA Immunoprecipitations were performed as described [45]. A total of 250 mL of cells was grown until $OD_{595} = 0.8$. Cells were cross-linked with 0.25% formaldehyde for 15 min at 30°C and the reaction was stopped with 0.25 M glycine for 5 min at room temperature. Cells were harvested by centrifugation, washed and resuspended in RIPA buffer and cell lysis / immunoprecipitation was performed as for ChIP followed by washing in RIPA buffer. A reversal buffer (10 mM Tris-HCl pH 6.8, 5 mM EDTA, 10 mM DTT, 1% SDS) was added to samples to reverse the cross-link at 70°C for 45 min. Samples were incubated at 37°C for 30 min in the presence of 40 μg of proteinase K and RNA was then extracted with phenol:chloroform and precipitated in 100% ethanol after treatment with DNaseI (New England Biolabs). RT-qPCR analyses were then performed as described above except that strand-specific primers and M-MLV RT (Invitrogen) were used instead of random primers.

Microarray experiments

Total RNA was extracted from in mid-logarithmic phase cells using hot phenol was purified using RNeasy kit (QIAGEN) and accessed for integrity using 2200 TAPE-station (Agilent Technologies). RNA was treated according to the Affymetrix total RNA labeling protocol (http://www.affymetrix.com) and hybridized to GeneChip *S. pombe* Tiling 1.0FR Arrays (Affymetrix) by the Affymetrix core facility at Karolinska Institutet (BEA). The each of the two biological replicates for WT and mutant were hybridized separately. For analysis the raw data (.CEL files) were first normalized in Tiling Analysis software (TAS) using one sample analysis quantile normalization plus scaling with bandwidth 100. Probe signals were assigned to *S.pombe* genome (Sanger 2004). Resulting files were imported into Podbat software (PMCID: PMC3161910) that was used for data quantification and visualization. To generate the list of up- and down-regulated elements, we filtered out false positives with signal-to-noise ratio (SNR) lower than 1 and set the threshold value 1.5 fold the average for WT (PMCID: PMC3512388).

Co-IP and *in vitro* GST pull-down assay of RNA

Immunoprecipiations were performed as described [46]: cells were disrupted with a Fastprep (MP) and proteins were precipitated on appropriately coated Dynabeads (Invitrogen) following the instructions of the manufacturer [47]. GST fusion proteins were expressed from pGEX4T1 and purified following the instructions of the manufacturer (GE Healthcare). The GST pull-down assay of RNA was performed as described [48]: 0.5 μg of GST-Mug187 or GST- were incubated with 1 μg of *in vitro* transcribed *rse1* (T7 *in vitro* transcription kit RiboMax, Promega. The T7 promoter was added to a G-block fragment (IDT) corresponding to *rse1*) for 1 hour at 4°C. After anti-GST immunoprecipitation, the samples were extracted with acidic phenol (pH 4.5) and precipitated with Ethanol 100%. The pellet was resuspended in 40 μl of water and 5 μl were used in Q-RT-PCR performed as described above on total (no IP) and immunoprecipitated samples.

RACE and poly-A RNA purification

RACE were performed using the SMARTer RACE 5′/3′ kit from Clonetech. Poly-adenylated RNAs were purified using the PolyATtract mRNA isolation system IV kit from Promega.

Chromatin Isolation by RNA precipitation

The protocol is based on previous work [25] and was adapted to yeast. A 250 mL culture was grown to OD_{595} 0.8 and crosslinked with 3% formaldehyde (final) for 30 minutes. After 20 minutes of incubation at RT, 13.5 mL of glycine 2.5 M were added. The pellet was treated with zymolyase to digest the cell wall and cells were lysed exactly as previously described for nucleosome scanning [29, 30]. The "chromatin" fraction was diluted 2X in hybridization buffer and 100 pmol of a set of tilling biotinylated probes (IDT) antisense to *rse1* (see Data S3) was added as described [25] overnight and recovered on MyOne streptavidine beads (Thermo). Elution was performed by addition of free biotin as described [49] and the eluted samples were separated by gradient PAGE (Bio-Rad) followed by silver staining (Bio-Rad).

Strand-specific CRISPR interference

In order to adapt the CRISPRi protocol to fission yeast, the pMZ289 [50] that harbors the wild-type Cas9 enzyme coding sequence was used to introduce the D10A and H840A mutations rendering the enzyme catalytically inactive by Quickchange mutagenesis. The region containing the Prrk1::sgRNA was then removed by SphI digestion and self-ligation, generating pDH753. A Leu2-based vector expressing the guide RNA was constructed by transferring a SphI-PstI fragment containing Prrk1::sgRNA [50] from pMZ289 to pART-I and this vector was used to introduce the DNA sequence corresponding to the guide RNA targeting the non-template strand.

rse1 CRISPRi: 5′-AGTGTAAGATTGCTTGCCACTGA-3′-NCC

The plasmids expressing the dead Cas9 and the appropriate sgRNA were co-transformed and selected on minimal media lacking leucine and uracile.

A recent work reported that the CRISPRi method is not always strand-specific and may redefine the transcriptional landscape [51]. In the present case, we found no evidence of such cases when analyzing the region by Northern blot (Figure 6). In addition, targeting the template strand of *rse1* (using the TTGACTTGTATAATCCCTCATTG guide) had no effect on either *rse1* or *ste11* (data not shown).

QUANTIFICATION AND STATISTICAL ANALYSIS

Statistical tests were performed using GraphPad Prism. Statistical significance was assessed using Student's t test comparing two means. Comparisons that are statistically significant are indicated as follows: ***$p < 0.001$; ** $p < 0.01$; *$p < 0.05$.

All the statistical analyses are described in the figure legends, including the statistical test used and the value of n that represents the number of independent replicates.

DATA AVAILABILITY

The accession number for the microarray data reported in this paper is Gene Expression Omnibus (NCBI-GEO): GSE89825.